Int. J. Nonlinear Anal. Appl. 14 (2023) 1, 3083–3096
ISSN: 2008-6822 (electronic)
http://dx.doi.org/10.22075/ijnaa.2022.27482.3616

Effect of nanoparticle loading on the polymer surface (Polyether-block-amide) in CO_2/CH_4 selectivity

Seyed Mohammad Faghih, Mahmoud Salimi*, Hossein Mazaheri

Department of Chemical Engineering, Arak Branch, Islamic Azad University, Arak, Iran

(Communicated by Madjid Eshaghi Gordji)

Abstract

In this research, we want to separate carbon dioxide gas from methane gas. Polymer (poly-ether-block-amide) has properties that absorb carbon dioxide well. Zeolite 4 A nanoparticles have fine pores and are proportional to the kinetic diameter of carbon dioxide, so they can act as a molecular sieve in the membrane, this nanoparticle was added to the polymer to obtain Pebax/4A nanocomposite membrane. Nanoparticles can improve carbon dioxide emissions and the thermal and mechanical stability of membranes. In this research, we want to investigate the effect of nano zeolite loading on the permeability and selectivity of carbon dioxide. By adding nanoparticles to the polymer, its structure was changed, so the nanocomposite membrane was evaluated by FESEM, BET, FTIR, and analyses. Finally, permeability, selectivity, diffusion coefficient, and solubility coefficient of carbon dioxide were calculated.

Keywords: CO_2 Separation, Membrane, Nanocomposite, Pebax, 4A Zeolite
2020 MSC: 35Q92

1 Introduction

Today, the chemical industry is trying to reduce some of the air pollutions by meeting environmental standards, carbon dioxide plays a key role in air pollution. Recently, the separation of gases by membranes has been considered because of the economics of this process, especially when high purity is not considered [4]. Researchers have recently used polyphosphates, polyamides, cellulose acetate, polyether urethane, polyurethane urethane urea, polyamide-polyester block copolymers, and polyvinylidene fluoride to separate the gas [7]. Lin and Freeman concluded that ethylene oxide (EO) has good selectivity for carbon dioxide. the choice of copolymers containing ethylene oxides, such as poly-ether-block-amide or PEBA, is suitable for achieving this goal [19]. Polyether-block-amid is an elastomeric thermoplastic whose chemical structure is shown in Figure 1.

Polyamide aliphatic (PA) and polyether (PE) form the hard and soft parts of this polymer, respectively. The hard part of the mechanical resistance and gas release is done through the PEO phase.

This polymer has good permeability and selectivity for carbon dioxide to methane [32] PEBA polymers are commercially produced and can also be converted into thin films. These polymers have several types of grades due to their different chemical structure, of which grade 1657 has the highest permeability [5]. One of the limitations of polymer

*Corresponding author
Email addresses: smfaghih@gmail.com (Seyed Mohammad Faghih), m-salimi@iau-arak.ac.ir (Mahmoud Salimi), h-mazaheri@iau-arak.ac.ir (Hossein Mazaheri)

Received: April 2022 *Accepted:* June 2022

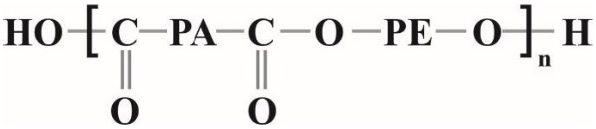

Figure 1: Chemical arrangement of PEBA polymers

membranes is the simultaneous increase in permeability and selectivity. Many solutions have been proposed by researchers to solve this problem, the most important of which is the creation of nanocomposite membranes. They are a new generation of membranes that include a polymer phase and filler phase [27]. Selectivity of polymer membranes and gas emission from filler pores can create good permeability and solubility in a membrane, simultaneously. One of the most suitable nanoparticles for the filler phase is zeolites. They have regular, fine, and controllable porosity and can act as molecular sieves [12, 29].

Type A zeolite is a known synthetic sample of the common chemical compound Na1. [AlO2.SiO2] $12.27H_2O$. This type of zeolite has 3 different groups 4A, 3A, and 5A, their difference is in the type of cation in the internal structure. 4A-type zeolite is commonly used to soften water and clean hazardous gases. Due to the pore diameter of this type of zeolite, it can increase gas emission and play a key role in the selectivity of carbon dioxide [12].

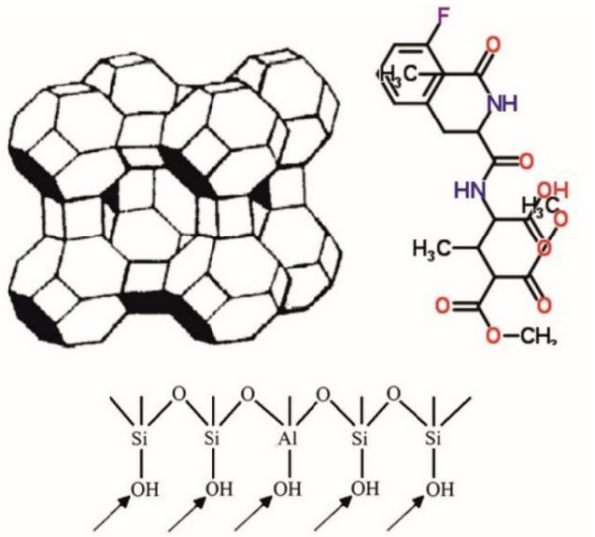

Figure 2: Three-dimensional and chemical structure of zeolite 4A [1, 30]

Much research has been done on the synthesis of Pebax-based membranes with a variety of nanoparticles, the results of which are summarized in Table 1.

Table 1: Results of some previous research

Ref.	Filler phase	Polymer	Temperature ($°C$)	Pressure (Bar)	Permeability (CO_2)	Selectivity
[2]	Zeolite 13X	Pebax1657	25	14	168.59	45
[11]	ZIF-8	Pebax1657/PE	60	25	758	16.1
[13]	DD3R	Pebax1074	55	20	188	38.5
[15]	ZIF-7	Pebax1657	35	30	150	40
[16]	NH2-CuBTC	Pebax1657	30	20	163	26.2
[18]	ZIF-7	Pebax1657	25	22	145	23
[34]	Zeolite NaY	Pebax1657	40	30	131.8	130.8
[33]	Zeolite NaX	Pebax1657/PES	25	2	45	121.5
[22]	ZIF-8	Pebax2533	35	–	1293	9

Pebax1657 and zeolite 4A have physical properties and chemical structure commensurate with the absorption of carbon dioxide. In this study, 1657 grade polyether block amide was selected as the polymer phase and 4A zeolite was

selected as the filler phase to modify the membrane structure.

2 Experimental

2.1 Materials

In this research, Pebax grade 1657 with a density of 1.14 gr/cm^3 made by the French company Arkema was used. This polymer contains 40% Wt. of polyamide-aliphatic as the hard part and 60% Wt. of polyethylene-oxide as the soft part. Zeolite 4A powder with a density of 0.5 gr/cm^3 and an average particle size of 250 to 500 nm was prepared from Behdash Iran Chemical Company. Also, ethanol solvent with a purity of 99.5% was purchased from Khorramshahr Alcohol Company of Iran. Methane and carbon dioxide gases with a purity of 99.9% were purchased and used from Khorramshahr Gas Oxygen Company.

2.2 Devices used in this research

XRD analysis with XRD Philips pw1730 device, FE-SEM analysis with TESCAN MIRA3 device, FTIR analysis with Thermos device model AVATAR, BET analysis with a special surface measuring device, Belsorp mini II from Microtrap Bel Corp Japan.

2.3 Nanocomposite membrane synthesis

For the membrane to have good mechanical strength, its thickness was selected to be 150 micrometers. The radius of the casting dish is 3.5 cm. According to the density of the polymer, the total membrane produced is 0.658 g. Accordingly, to achieve a 5% weight of zeolite in the membrane, we first heat 0.033 g of zeolite powder at 70°C for 4 hours to dry completely [17]. The dried zeolite and 12.5 g of solvent (Ethanol 70%, Water 30%) were placed on a magnetic stirrer for 3 hours at 45°C [6].

The resulting solution was placed in an ultrasonic device with a temperature of 45°C, a frequency of 42 kHz, and a power of 50 watts for 10 minutes. this operation was performed to de-bubble the solution. To this solution, 0.625 g of Pebax 1657 granules were added and heated in an oil bath and water reflex for 3 hours. According to the solvent type, the temperature of this bath was selected to be 120°C.

The petri dish was heated to 80°C. this action prevented damage to the morphology of the solution before casting [23]. The solution pours into a Petri dish and in an oven at 35°C for 30 hours place for dried. To ensure complete evaporation of the solvent, this time the petri dish was heated for 2 hours in a vacuum oven at 35°C and the membrane fabrication operation was completed.

Membranes with concentrations of 0, 10, 18, and 35% by weight of zeolite were made by the same method. The thickness of the membranes was measured by the Japanese digital thickness gauge GT-313-A1 in Japan and named according to Table 2.

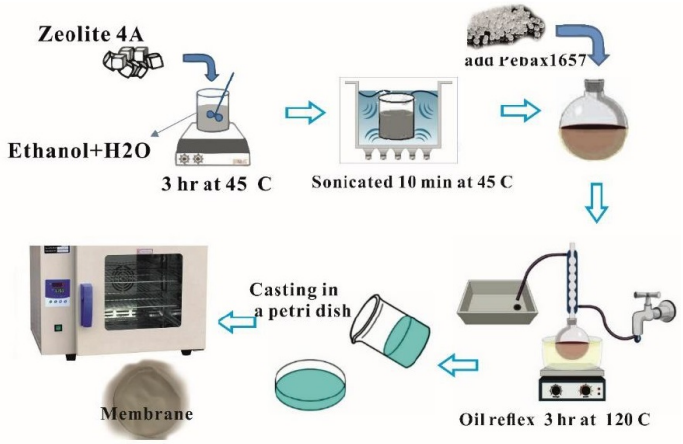

Figure 3: Nanocomposite membrane synthesis steps

Table 2: Percentage by weight of polymer and filler membranes created.

ID	Pebax %Wt.	4A %Wt.	Solvent (gr)	Thickness (μm)
PA-0	100	0	12.5	138
PA-5	95	5	12.5	140
PA-10	90	10	12.5	139
PA-18	82	18	12.5	142
PA-35	65	35	12.5	141

2.4 Permeability measurement

The gas permeability measuring system was constructed as a fixed volume. This system can measure permeability at different pressures. The membrane module was made using pure stainless steel. Rubber rings were used on both sides of the membrane to prevent gas leakage. Also, a thin metal mesh made of steel was used to prevent the membrane from tearing and to withstand pressure. The effective surface area of the membrane in this system is 17.71 cm^2. Permeability tests were performed at $30°C$ and pressure of 3 bar, each with three replications.

Gas permeability was calculated by the constant volume method by Equation (2.1) and reported in the Barrer unit:

$$P(Barrer) = \frac{273.15 \times 10^{10} LV}{760 \times 76 \left(AT\frac{Po}{14.7}\right)} \frac{dP}{dt} \tag{2.1}$$

1 Barrer=10-10 cm3 (STP)·cm/ (cm2. s. cmHg).

In this equation, $(cm^3)V$ is the volume of the reservoir behind the membrane, $L(cm)$ is the thickness of the membrane, $A(cm^2)$ is the effective surface of the membrane, $T(K)$ is the temperature, $Po(psia)$ is the inlet gas pressure, and (bar/s) is (dP/dt) is the pressure change over time [3, 9].

The ideal selectivity of gases was calculated using Equation (2.2) [10, 20]:

$$\alpha_{CO_2/CH_4} = \frac{P_{CO_2}}{P_{CH_4}} \tag{2.2}$$

The CO_2 diffusion coefficient was calculated according to the following equation using the Time-lag method [20]:

$$D_{CO_2} = \frac{L^2}{6\theta} \tag{2.3}$$

In Equation (2.3), time θ was obtained by extrapolating the linear part of the pressure graph in terms of time and its intersection with the time axis.

The solubility coefficient of gases was calculated according to Equation (2.4) [20]:

$$S_A = \frac{P_A}{D_A} \tag{2.4}$$

Permeability, selectivity, solubility coefficient, and diffusion coefficient of synthesized membranes are listed in Table 3.

Table 3: Permeability, diffusion coefficient, solubility coefficient and selectivity

ID	P_{CO_2}	P_{CH_4}	$\frac{CO_2}{CH_4}$	D_{CO_2}	S_{CO_2}
PA-0	56	3.5	16.00	48	1.17
PA-5	63.1	3.8	16.61	50.1	1.26
PA-10	69.6	4.16	16.73	52.3	1.33
PA-18	67.8	4.06	16.70	51.5	1.32
PA-35	66.8	4.07	16.41	50.9	1.31

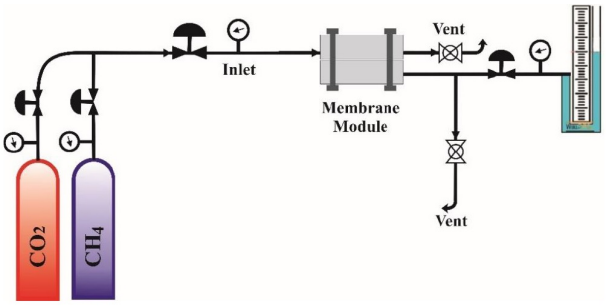

Figure 4: Permeability measurement system

3 Results and Discussion

3.1 Analysis of X-ray diffraction (XRD)

X-ray diffraction (XRD) test was used to evaluate the crystal structure of the synthesized membranes. XRD analysis was performed from 10 to 80 degrees and the device step was 0.05 degrees per second. As can be seen in Figure 5, the zeolite phase formed by the major peaks of the particles at 20.5 and 42.5° corresponds to the X-ray reflection of the polymer crystal structure and the plates 24, 27, 31 and 43° to the crystal structure of the nanoparticles [14, 21].

The weaker peaks observed at other angles are inevitable, they are related to impurities and unknown phases. in general, surface modification with non-crystalline agents reduces the crystallinity of the base particles. With the presence of zeolite in Pebax substrate, the molecular free volume increases, so the overall hardness of this copolymer decreases, and its softening affects the further penetration of gas.

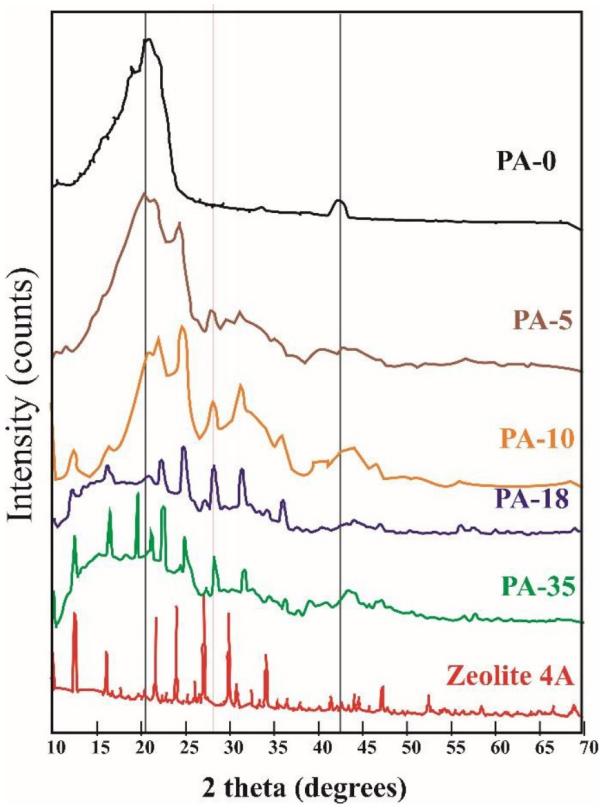

Figure 5: X-ray diffraction (XRD)

3.2 Analysis of infrared Fourier transforms (FTIR)

This analysis was performed in the range of 600 to 4000 (cm-1) on the membranes. As shown in Figure 6, the peak at 1635 cm-1 is the tensile vibrations ($O = C$) of carbonyl. The peak in wave number 1730 cm-1 is attributed to another carbonyl group, both of which are in the hard phase. The peak in 1538 cm-1 is related to the $N - H$ flexural vibration in polyamide parts, and the peak in 3290 cm-1 is related to the tensile vibration ($N - H$) [28]. Peaks 2861 cm-1 and peaks 1460 cm-1 were also associated with $C - H$ tensile and flexural vibrations, respectively. These results were in good agreement with other studies [21].

In the 4A zeolite spectrum, the broad absorption band at 3300 cm-1 to 3600 cm-1 and the absorption band at 1650 cm-1 belong to the hydroxyl ($-OH$) groups due to the presence of water in the zeolite. The absorptions in 995 wavelengths are related to the bending vibrations of $O - Si$ or $O - Al$ [35].

As the zeolite load increased, the peak intensity increased to 3300 to 3500 cm-1. This change may be due to the increased zeolite load. Zeolite adsorption bands overlap with the corresponding bands in the Pebax spectrum. this issue is more evident in the range of 1000 cm-1, which intensifies with an increasing percentage of zeolite due to the joint effect of $Si - O$ or $Al - O$ bonds on zeolite.

Finally, the Pebax and zeolite functional groups did not form a chemical bond, but the crystallinity in the 35% by weight membrane was greatly reduced.

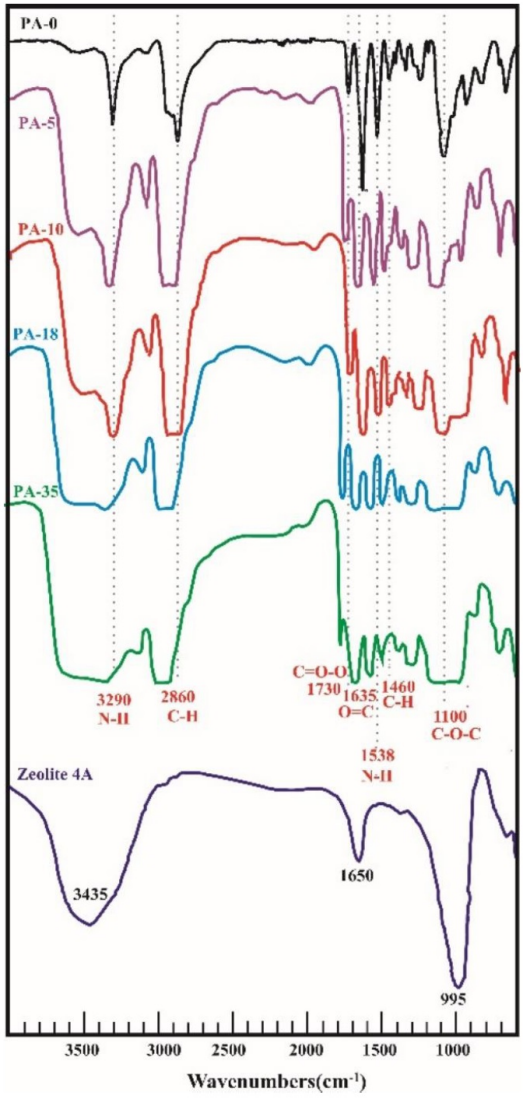

Figure 6: Fourier transform infrared spectroscopy (FTIR).

3.3 Imaging by method scanning electron microscopy (FE-SEM)

The penetration of gases in polymer membranes depends on their morphology. FE-SEM imaging was performed to examine the structure of the membranes. Figure 7 shows the FE-SEM images of pure Pebax membranes mixed with different percentages of zeolite. Pure Pebax membrane has a uniform surface but small cracks are observed on it, these cracks are probably due to the drying operation of the membrane. According to these images, it can be seen that the morphology of the membrane surface changes with the addition of zeolite to the Pebax. With increasing zeolite, more changes in surface morphology are seen.

Loading in 18% and 35% of zeolite samples indicates the accumulation of particles and clumping at several points on the polymer surface. Imaging of the cross-section of the pure Pebax membrane shows a thickness of 138 μm. at several points on the polymer surface. Imaging of the cross-section of the pure Pebax membrane shows a thickness of 138 μm.

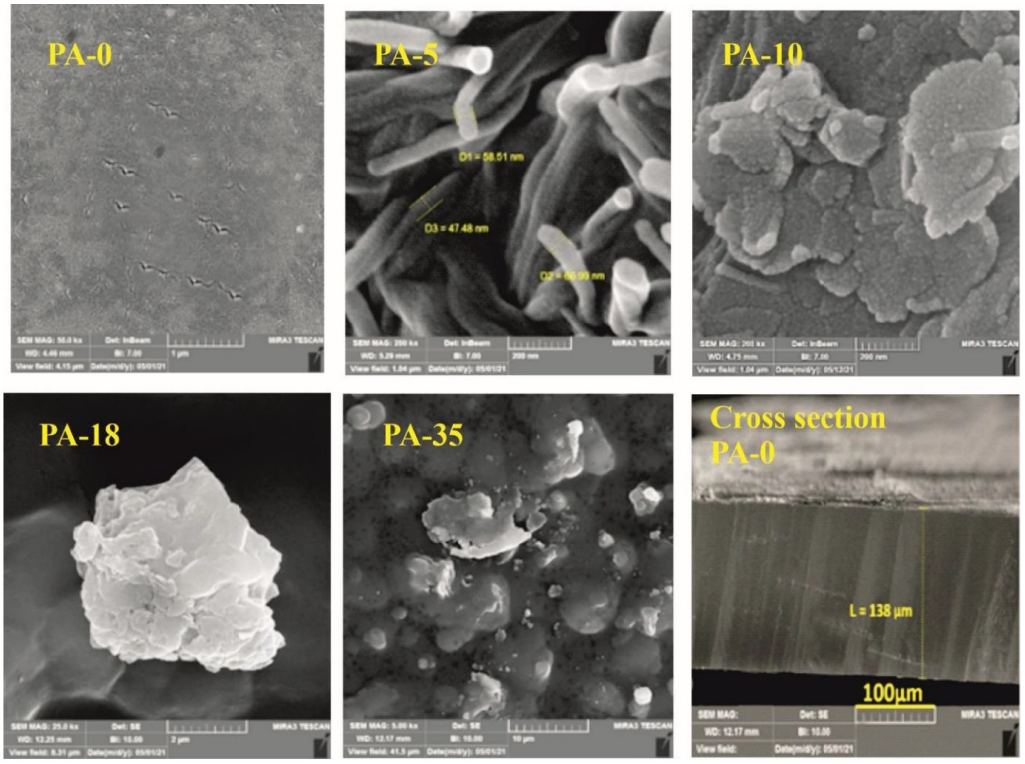

Figure 7: Scanning Electron Microscope (FE-SEM).

3.4 Surface measurement specificity and porosity (BET)

BET analysis was performed to determine some physical properties such as surface area, pore-volume, and pore surface. Nitrogen adsorption and desorption isotherms at 77 K were calculated for all samples. After loading the filler in membrane number 10, its specific surface area was 85% higher than pure polymer membrane. This parameter is very effective in increasing absorption. The data obtained from this analysis were listed in Table 4.

Table 4: Results of BET analysis

ID	**Total pore volume** $(p/p0 = 0.990)[cm^3g^{-1}]$	$a_{s,BET}$ $[m^2g^{-1}]$
PA-0	0.0044627	2.596
PA-5	0.013377	3.5192
PA-10	0.0043634	4.8115
PA-18	0.0040921	3.8212
PA-35	0.0039795	1.9897

3.5 The effect of adding nanoparticles

Figure 8 shows that the permeability of carbon dioxide in membranes with 5 and 10% by weight of zeolite is slightly better than that of the pure membrane.

several factors can increase the permeability of carbon dioxide. The first factor according to the results of the BET test is the increase of penetration channels due to the increase in the contact surface, the second factor can be the creation of hydrogen bonds between nanoparticles and polymers, which plays an important role in determining fuzzy separation [6]. Loading of nanoparticles reduces the density of polymer chains and weakens the hydrogen bond between them, which leads to an increase in the free volume of the polymer.

The amount of fractional free volume (FFV) within polymers is often calculated according to Equation (3.1) [8]:

$$FFV = \frac{V_{SP} - V_0}{V_{SP}} \tag{3.1}$$

V_{SP} is the specific volume of the polymer, and V_0 is the volume occupied by the polymer chains, which is calculated by Equation (3.2) [8].

$$V_0 = 1.3V_W \tag{3.2}$$

V_W is the volume of van der Waals calculated by the group correlation method. According to this equation, increasing FFV increases the penetration of gas molecules and ultimately improves permeability.

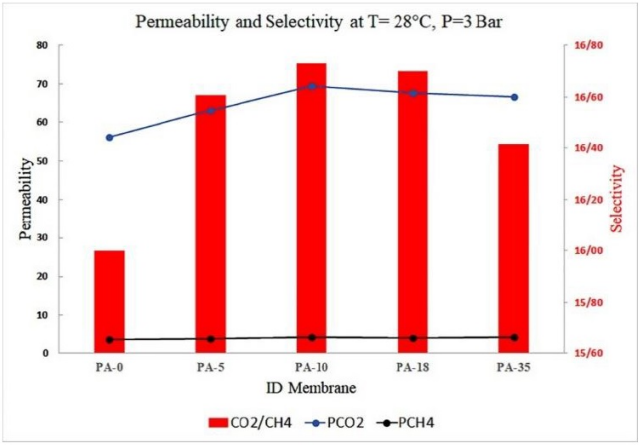

Figure 8: Permeability and selectivity of CO_2 and CH_4.

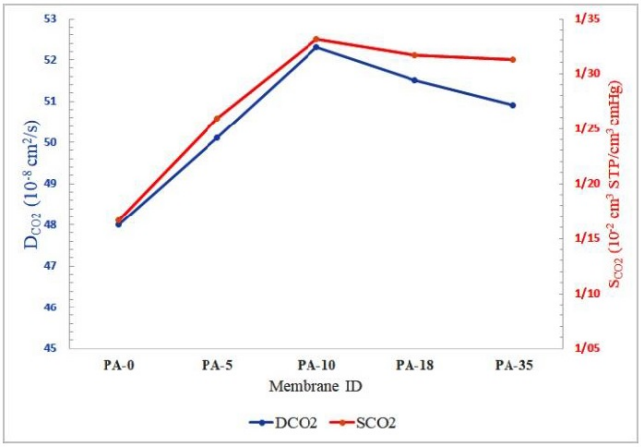

Figure 9: Diffusion coefficient, Solubility coefficient of CO_2

3.6 Theoretical calculations and mass transfer model

Regarding the modeling of asymmetric membranes used for gas separation, limited studies have been carried out so far, among which Rangarajan and his colleagues' research in 1984 can be mentioned [25]. In this research, the pore flow model alone is used to model the performance of the asymmetric membrane. In 1988, following Rang Rajan's research, Tremblay used the Simplex method to determine the unknown characteristics of the presented model [25].

In 1990, Wang and his colleagues [31] presented a model to determine the characteristics of an asymmetric membrane with low surface porosity of small holes and claimed that the transfer of gases in the holes is carried out only by Knudson-viscous currents. The total flux includes not only these two currents but also Dissolution-permeation also includes the passage of gases through the compressed part of the surface.

In addition, they assumed the permeability coefficient to be independent of the pressure, in order to determine the characteristics of the membrane, the total permeability of the desired gas was measured at different pressures, then the total permeability was measured according to the average pressure of the clay, and finally, the value of the total permeability of the gas at zero pressure (according to the resulting figure) They extrapolated. In continuation of the research done in this field, in this research, an attempt has been made to present a general model by considering all aspects. In this research, the asymmetric membranes in question are membranes with low surface porosity for which three separate areas are considered, and these areas of electrical similarity of this type of membranes are specified in the figure 10.

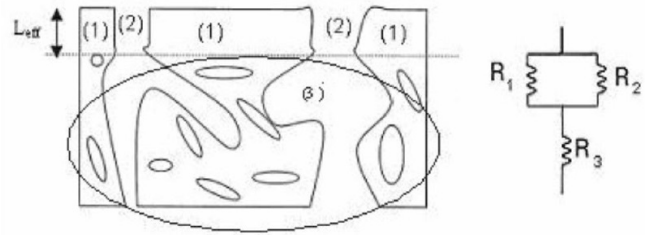

Figure 10: Asymmetric membrane and its equivalent electric circuit

These areas are respectively: the compact part of the surface area (area No. 1) with the thickness of L_{eff} (the effective separation thickness), the porosity of the surface area (area No. 2), the completely porous network (area No. 3).

According to the previous models presented for asymmetric membranes, it is assumed that region 3 specified in figure 10 has a very high porosity and its resistance against the passage of gas flow is negligible ($R3 \cong 0$), so the gas flow when passing through the membranes are faced with two parallel resistances, according to the electrical analogy, the total gas flow through the membrane is expressed as follows.

$$I_{total} = I_1 + I_2, \quad Q_{total} = Q_1 + Q_2 \tag{3.3}$$

where Q_{total} is the total gas flow rate, Q_1 is the gas flow passing through the dense part and Q_2 is the gas flow rate passing through the pores of the membrane surface. Based on the mentioned model for porous media, the total gas flow through the pores is calculated according to the following equation:

$$Q_2 = \frac{N_t}{L}(G_1 I_1 + G_2 I_2 + G_3 I_3)\Delta p + A_2' \frac{I_4}{I_5} p \Delta p. \tag{3.4}$$

Considering that the passage of gas through the compressed part of the surface region follows the dissolution-permeation mechanism, therefore, the flow rate for this state can be expressed as follows:

$$Q_1 = P S_1 \frac{\Delta p}{L_{eff}} \tag{3.5}$$

where S_1 is the area of the compressed part of the surface area, Δp is the pressure difference, L_{eff} is the thickness of the surface area and p is the permeability coefficient. From the combination of equations (3.4) and (3.5) of the total gas flow rate through the asymmetric porous membrane, its permeability relation is expressed as follows:

$$Q_{total} = \frac{N_t}{L}(G_1 I_1 + G_2 I_2 + G_3 I_3)\Delta p + A_2' \frac{I_4}{I_5} \bar{p} \Delta p + P S_1 \frac{\Delta p}{L_{eff}} \tag{3.6}$$

$$J_{total} = \frac{Q_{total}}{\Delta p S_{total}} \tag{3.7}$$

$$J_{total} = \frac{N_t}{LS_{total}}(G_1 I_1 + G_2 I_2 + G_3 I_3) + \frac{A_2'}{S_{total}}\frac{I_4}{I_5}\bar{p} + \frac{S_1}{S_{total}}\frac{P}{L_{eff}} \tag{3.8}$$

where S_{total} is the surface of the whole membrane and J_{total} is the permeability of the whole membrane. In addition, surface porosity is based on the following relationship.

$$\varepsilon = \frac{S_2}{S_{total}} \longrightarrow 1 - \varepsilon = \frac{S_1}{S_{total}} \tag{3.9}$$

where S_2 is the pore surface and ε is the surface porosity. In asymmetric membranes suitable for gas separation usually $\varepsilon < 10^{-5}$

$$\frac{S_1}{S_{total}} = 1 - \varepsilon \cong 1 \longrightarrow S_1 \cong S_{total} \tag{3.10}$$

$$J_{total} = A_1(G_1 I_1 + G_2 I_2 + G_3 I_3) + A_2\frac{I_4}{I_5}\bar{p} + \frac{P}{L_{eff}} \tag{3.11}$$

$$A_1 = \frac{N_t}{LS_{total}} \tag{3.12}$$

$$A_2 = \frac{A_2'}{S_{total}} \tag{3.13}$$

In equation (3.11), the values of G_1 and G_2 are constant and G_3 and P depend on the pressure. And L_{eff} is the structural characteristic of the membrane, whose value is determined based on SEM images. $I_1, I_2, I_3, I_4, I_5, A_2, A_1$ are the characteristics of the above relationship and must be determined. Therefore, equation (3.11) is a non-linear function of pressure. If the values of pure gas permeability (J_{total}) at different pressures are known, non-linear regression can be used to determine the unknowns of the relationship.

3.6.1 Determining unknown characteristics of the model

According to the relation (3.11), the permeability of a pure gas is a non-linear function of the average pressure, in order to calculate its value, the unknowns A_2, A_1, r, σ must be determined. For this purpose, if the values of pure gas permeability (J_{total}) (dependent variable) at medium pressures $\bar{p}$ (independent variable) are known, by using "non-linear regression" the best curve that can be fitted to the existing experimental points can be determined. As a result, the characteristic values are unknown.

To perform nonlinear regression, a function can be defined as the sum of squares of the difference between the permeability calculated by equation (3.11) (J_{calc}) and the experimental permeability (J_{exp}).

$$SS_R = \sum_{i=0}^{n}(J_{exp\ i} - J_{calc\ i})^2 \tag{3.14}$$

where n is the number of experimental data. The SS_R function is considered as the target function by using a suitable optimization method, the values of the unknown parameters $A_2, A_1 r, \sigma$, which minimize the value of the target function, are calculated.

The method of determining characteristics: since the optimization methods need a starting point to perform calculations, for this reason, the order of numbers that can be assigned to the existing characteristics should be determined. Each of them is discussed below.

$\bar{r}$ Considering that the value of the maximum radius of the holes is known, then the average radius is a value in the range $(0, r\,\max)$.

(σ): Based on the definition of probability density $f(r) = f(N(r))/N_t$ the following relationship is established.

$$\int_0^{\infty} f(r)dr = 1. \tag{3.15}$$

If the probability of the presence of holes with a radius larger than $r_{\max}$ is assumed to be zero, then:

$$\int_0^{r_{\max}} f(r)dr = 1. \tag{3.16}$$

As a result, the deviation from the standard σ and r accept the values that the equation (3.16) is established.

(A_2, A_1): assuming that σ and r are known, we replace A_2 and A_1 as independent variables X_1 and X_2 and J_{total} as dependent variable Y. The relationship is expressed as follows.

$$Y_i = a_i X_1 + b_i X_2 + c_i \tag{3.17}$$

$$a_i = G_1 I_{1,i} + G_2 I_{2,i} + G_3 I_{3,i} \tag{3.18}$$

$$b_i = \frac{I_{4,i}}{I_{5,i}} \bar{p}_i \tag{3.19}$$

$$c_i = \frac{P_i}{L_{eff}} \tag{3.20}$$

c_i, b_i, a_i are constant values in medium pressure. So

$$SS_R = \sum_{i=1}^{n} \left[Y_{exp\ i} - (a_i X_1 + b_i X_2 + c_i) \right]^2 \tag{3.21}$$

$$\frac{\partial SS_R}{\partial X_1} = 0, \quad \frac{\partial SS_R}{\partial X_2} = 0,$$

$\min SS_R(A_1, A_2, r, \sigma)$ subject to:

$$LBA_1 < A_1 < UBA_1$$

$$LBA_2 < A_2 < UBA_2$$

$$0 < r < r_{\max} :$$

$$\int_0^{r_{\max}} \frac{N(r)}{N_t} dr = 1. \tag{3.22}$$

According to the order obtained for A_2 and A_1, arbitrary values of the beginning and the end of the corresponding interval are considered. To determine the optimal point of the existing function, an optimization method whose scope can be limited is needed. For this reason, Newton Quasi method, Fmincon function of Matlab software, which has the ability to accept nonlinear linear constraints, has been used. With the Newton Quasi method for different starting points, different minima are obtained (local minimums). For this reason, the combination of the Newton Quasi method and the genetic algorithm, which is actually considered a type of combination algorithm, has been used.

Based on the genetic algorithm, from different areas of the objective function domain, populations of selected starting points for each of the points in each population, using the Quasi Newton method, the optimal point is calculated by comparing the obtained answers, the lowest value as the point The optimum of the mentioned population is stored after applying this method for all populations, the main optimal point is determined by comparing the stored values.

4 Conclusion

In this study, the polymer membrane of Pebax 1657 composite matrix and zeolite 4A particles were fabricated by solvent-evaporation casting method, and its performance in CO_2/CH_4 separation at a feed pressure of 3 bar was investigated. The results of the FTIR test ruled out the formation of a new chemical bond between the zeolite and the polymer. But FE-SEM images showed that in membranes amount of than 18%, the nanoparticles were not well dispersed in the polymer and clumped in some places, a problem that negatively affected permeability. BET analysis shows that increasing nanoparticles by up to 10% by weight can have a good effect on increasing the gas-membrane contact surface.

Figures 8 and 9 of the permeability test data show that by increasing the nanoparticle to 10% by weight, we can have a higher permeability than the pure membrane in the nanocomposite. Also, its penetration coefficient and solubility coefficient were higher, but compared to similar studies, a lower penetration coefficient was obtained [8, 24]. The most important parameter affecting the gas penetration is the thickness of the membrane, it seems that due to the thickness of the membrane has increased the mass transfer resistance.

The reduction of diffusion coefficients and solubility at 18 and 35% by weight can be due to particle aggregation, clumping, and the formation of a common level between the particles and the polymer. Also, a small amount of solvent in the polymer may clog some pores and reduce permeability.

Robeson reported a comprehensive analysis of the two-component permeability of gases. He proved that high-permeability membranes often have low selectivity for gas pairs. In the permeability selectivity diagram, he set a limit for polymer membranes called the Robeson upper limit. The closer the polymer membrane is to this range, the better its performance and the more suitable it is for industrialization [26].

The performance of the membranes made in this study was compared with the Robeson diagram in Figure 11. in this diagram, the nanocomposites were placed below the Robeson line. According to the successful research that has been done in this field, parameters such as the type and amount of solvent, as well as the dissolution temperature and drying time, may not have been selected correctly in the synthesis method of this membrane. The correct choice of these variables seems to be very effective in making membranes with uniform morphology.

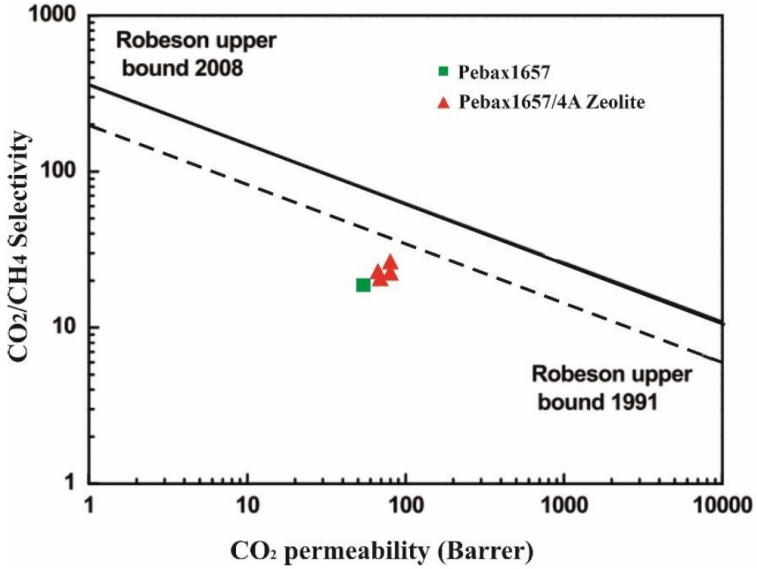

Figure 11: Robeson upper limit chart

References

[1] J. Ahmad and M.-B. Hägg, *Preparation and characterization of polyvinyl acetate/zeolite 4A mixed matrix membrane for gas separation*, J. Membrane Sci. **427** (2013), 73–84.

[2] M. Asghari, M. Mosadegh and H.R. Harami, *Supported PEBA-zeolite 13X nano-composite membranes for gas separation: Preparation, characterization and molecular dynamics simulation*, Chemic. Eng. Sci. **187** (2018), 67–78.

[3] N. Azizi, M. Isanejad, T. Mohammadi and R.M. Behbahani, *Effect of TiO2 loading on the morphology and CO2/CH4 separation performance of PEBAX-based membranes*, Front. Chem. Sci. Engin. **13** (2019), no. 3, 517–530.

[4] A. Brunetti, F. Scura, G. Barbieri and E. Drioli, *Membrane technologies for CO2 separation*, J. Membrane Sci. **359** (2010), no. 1–2, 115–125.

[5] P.M. Budd, N.B. McKeown, D. Fritsch, Y. Yampolskii and V. Shantarovich, *Gas permeation parameters and other physicochemical properties of a polymer of intrinsic microporosity (PIM-1)*, J. Taiwan Inst. Chem. Engin. (2010), 29–42.

[6] A.H.S. Dehaghani, S. Rashidian, V. Pirouzfar and C.H. Su, *The novel composite membranes containing chloride and acid functionalized multiwall carbon nanotube fillers for gas separation*, Colloid Polymer Sci. **299** (2021), no. 12, 1933–1944.

[7] A. Ehsani and M. Pakizeh, *Synthesis, characterization and gas permeation study of ZIF-11/Pebax® 2533 mixed matrix membranes*, Journal of the Taiwan Instit. Chem. Engin. **66** (2016), 414–423.

[8] N. Habib, Z. Shamair, N. Tara, A.S. Nizami, F.H. Akhtar, N.M. Ahmad, M.A. Gilani, M.R. Bilad and A.L. Khan, *Development of highly permeable and selective mixed matrix membranes based on Pebax®1657 and NOTT-300 for CO2 capture*, Separ. Purific. Technol. **234** (2020), 116101.

[9] H. Hosseinzadeh Beiragh, M. Omidkhah, R. Abedini, T. Khosravi and S. Pakseresht, *Synthesis and characterization of poly (ether-block-amide) mixed matrix membranes incorporated by nanoporous ZSM-5 particles for CO2/CH4 separation*, Asia-Pacific J. Chemic. Eng. **11** (2016), no. 4, 522–532.

[10] M. Jamshidi, V. Pirouzfar, R. Abedini and M.Z. Pedram, *The influence of nanoparticles on gas transport properties of mixed matrix membranes: An experimental investigation and modeling*, Korean J. Chemic. Eng. **34** (2017), no. 3, 829–843.

[11] A. Jomekian, R.M. Behbahani, T. Mohammadi and A. Kargari, *CO2/CH4 separation by high performance co-casted ZIF-8/Pebax 1657/PES mixed matrix membrane*, J. Natural Gas Sci. Engin. **31** (2016), 562–574.

[12] M.S. Jyothi, K.R. Reddy, K. Soontarapa, S. Naveen, A.V. Raghu, R.V. Kulkarni, D.P. Suhas, N.P. Shetti, M.N. Nadagouda and T.M. Aminabhavi, *Membranes for dehydration of alcohols via pervaporation*, J. Environ. Manag. **242** (2019), 415–429.

[13] F. Karamouz, H. Maghsoudi and R. Yegani, *Synthesis of high-performance Pebax®-1074/DD3R mixed-matrix membranes for CO2/CH4 separation*, Chem. Eng. Tech. **41** (2018), no. 9, 1767–1775.

[14] E. Khoramzadeh, M. Mofarahi and C.-H. Lee, *Equilibrium adsorption study of CO2 and N2 on synthesized zeolites 13X, 4A, 5A, and Beta*, J. Chemic. Eng. Data **64** (2019), no. 12, 5648–5664.

[15] A. Khoshkharam, N. Azizi, R.M. Behbahani and M.A. Ghayyem, *Separation of CO2 from CH4 using a synthesized Pebax-1657/ZIF-7 mixed matrix membrane*, Petroleum Sci. Technol. **35** (2017), no. 7, 667–673.

[16] T. Khosravi, M. Omidkhah, S. Kaliaguine and D. Rodrigue, *Amine-functionalized CuBTC/poly(ether-b-amide-6) (Pebax® MH 1657) mixed matrix membranes for CO2/CH4 separation*, Canadian J. Chemic. Eng. **95** (2017), no. 10, 2024–2033.

[17] E. Kianfar, V. Pirouzfar and H. Sakhaeinia, *An experimental study on absorption/stripping CO2 using Monoethanol amine hollow fiber membrane contactor*, J. Taiwan Instit. Chem. Engin. **80** (2017), 954–962.

[18] T. Li, Y. Pan, K.V. Peinemann and Z. Lai, *Carbon dioxide selective mixed matrix composite membrane containing ZIF-7 nano-fillers*, J. Membrane Sci. **425** (2013), 235–242.

[19] H. Lin, B.D. Freeman, S. Kalakkunnath and D.S. Kalika, *Effect of copolymer composition, temperature, and carbon dioxide fugacity on pure-and mixed-gas permeability in poly (ethylene glycol)-based materials: Free volume interpretation*, J. Membrane Sci. **291** (2007), no. 1–2, 131–139.

[20] M. Monteleone, E. Esposito, A. Fuoco, M. Lanč, K. Pilnáček, K. Friess, C.G. Bezzu, M. Carta, N.B. McKeown and J.C. Jansen, *A novel time lag method for the analysis of mixed gas diffusion in polymeric membranes by on-line mass spectrometry: Pressure dependence of transport parameters*, Membranes **8** (2018), no. 3, 73.

[21] R.S. Murali, A.F. Ismail, M.A. Rahman and S. Sridhar, *Mixed matrix membranes of Pebax-1657 loaded with 4A zeolite for gaseous separations*, Separ. Purific. Technol. **129** (2014), 1–8.

[22] V. Nafisi and M.-B. Hägg, *Development of dual layer of ZIF-8/PEBAX-2533 mixed matrix membrane for CO2 capture*, J. Membrane Sci. **459** (2014), 244–255.

[23] A.V. Raghu, G.S. Gadaginamath, N.T. Mathew, S.B. Halligudi and T.M. Aminabhavi, *Synthesis and characterization of novel polyurethanes based on 4, 4'-[1, 4-phenylenedi-diazene-2, 1-diyl] bis (2-carboxyphenol) and 4, 4'-[1, 4-phenylenedi-diazene-2, 1-diyl] bis (2-chlorophenol) hard segments*, React. Funct. Polymers **67** (2007) no. 6, 503–514.

[24] M.M. Rahman, S. Shishatskiy, C. Abetz, P. Georgopanos, S. Neumann, M.M. Khan, V. Filiz and V. Abetz, *Influence of temperature upon properties of tailor-made PEBAX® MH 1657 nanocomposite membranes for post-combustion CO2 capture*, J. Membrane Sci. **469** (2014), 344–354.

[25] R. Rangarajan, M.A. Mazid, T. Matsuura and S. Sourirajan, *Permeation of pure gases under pressure through*

asymmetric porous membranes, membrane characterization and prediction of performance, Ind. Eng. Chem. Process Des. Dev. **23** (1984), 79–87.

[26] L.M. Robeson, *The upper bound revisited*, J. Membrane Sci. **320** (2008), no. 1-2, 390–400.

[27] A.H. Saeedi Dehaghani, V. Pirouzfar and A. Alihosseini, *Novel nanocomposite membranes-derived poly(4-methyl-1-pentene)/functionalized titanium dioxide to improve the gases transport properties and separation performance*, Polymer Bull. **77** (2020), no. 12, 6467–6489.

[28] D.P. Suhas, T.M. Aminabhavi, H.M. Jeong and A.V. Raghu, *Hydrogen peroxide treated graphene as an effective nanosheet filler for separation application*, RSC Adv. **5** (2015), no. 122, 100984–100995.

[29] D.P. Suhas, T.M. Aminabhavi and A.V. Raghu, *Mixed matrix membranes of H-ZSM5-loaded poly (vinyl alcohol) used in pervaporation dehydration of alcohols: Influence of silica/alumina ratio*, Polymer Eng. Sci. **54** (2014), no. 8, 1774–1782.

[30] L.A. Tuyen, E. Szilágyi, E. Kótai, K. Lázár, L. Bottyán, T.Q. Dung, L.C. Cuong, D.D. Khiem, P.T. Phuc, L.L. Nguyen and P.T. Hue, *Structural effects induced by 2.5MeV proton beam on zeolite 4A: Positron annihilation and X-ray diffraction study*, Radi. Phys. Chem. **106** (2015), 355–359.

[31] D. Wang, K. Li and W.K. Teo, *Effects of temperature and pressure on gas permselection properties in asymmetric membranes*, J. Membrane Sci. **105** (1995), no. 1–2, 89–101.

[32] M. Zanetti, G. Camino, R. Thomann and R. Mülhaupt, *Synthesis and thermal behaviour of layered silicate–EVA nanocomposites*, Polymer **42** (2001), no. 10, 4501–4507.

[33] K. Zarshenas, A. Raisi and A. Aroujalian, *Mixed matrix membrane of nano-zeolite NaX/poly (ether-block-amide) for gas separation applications*, J. Membrane Sci. **510** (2016), 270–283.

[34] Y. Zheng, Y. Wu, B. Zhang and Z. Wang, *Preparation and characterization of CO2-selective Pebax/NaY mixed matrix membranes*, J. Appl. Polymer Sci. **137** (2020), no. 9, p. 48398.

[35] W. Zou, H. Bai, L. Zhao, K. Li and R. Han, *Characterization and properties of zeolite as adsorbent for removal of uranium(VI) from solution in fixed bed column*, J. Radioanal. Nuclear Chem. **288** (2011), 779–788.